



Contents lists available at ScienceDirect

Bioorganic & Medicinal Chemistry Letters

journal homepage: www.elsevier.com/locate/bmcl



Inhibitors of hepatitis C virus polymerase: Synthesis and characterization of novel 2-oxy-6-fluoro-*N*-((*S*)-1-hydroxy-3-phenylpropan-2-yl)-benzamides

Cliff C. Cheng^{a,*}, Gerald W. Shipp Jr.^a, Zhiwei Yang^{a,†}, Noriyuki Kawahata^{a,‡}, Charles A. Lesburg^b, José S. Duca^b, Jamie Bandouveres^a, Jack D. Bracken^a, Chuan-kui Jiang^c, Sony Agrawal^c, Eric Ferrari^c, H.-C. Huang^c

^a Department of Lead Discovery, Merck Research Laboratories, 320 Bent Street, Cambridge, MA 02141, United States

^b Department of Drug Design, Merck Research Laboratories, 2015 Galloping Hill Road, Kenilworth, NJ 07033, United States

^c Department of Infectious Diseases, Merck Research Laboratories, 2015 Galloping Hill Road, Kenilworth, NJ 07033, United States

ARTICLE INFO

Article history:

Received 14 October 2009

Revised 11 February 2010

Accepted 11 February 2010

Available online 18 February 2010

Keywords:

HCV NS5B polymerase

Hepatitis C virus

Palm site inhibitors

Replicon

Antiviral

ALIS: automated ligand identification system

Structure based drug design (SBDD)

ABSTRACT

SAR exploration from an initial hit, (*S*)-*N*-(2-cyclohexylethyl)-2-fluoro-6-(2-(1-hydroxy-3-phenylpropan-2-ylamino)-2-oxoethoxy)benzamide (**1**), identified using our proprietary automated ligand identification system (ALIS),¹ has led to a novel series of selective hepatitis C virus (HCV) NS5B polymerase inhibitors with improved in vitro potency as exemplified by (*S*)-2-fluoro-6-(2-(1-hydroxy-3-phenylpropan-2-ylamino)-2-oxoethoxy)-*N*-isopentyl-*N*-methylbenzamidocarboxamide (**41**) (IC₅₀ = 0.5 μM). The crystal structure of an analogue (**44**) was solved and provided rationalization of the SAR of this series, which binds in a distinct manner in the palm domain of NS5B, consistent with biochemical analysis using enzyme mutant variants. These data warrant further lead optimization efforts on this novel series of non-nucleoside inhibitors targeting the HCV polymerase.

© 2010 Elsevier Ltd. All rights reserved.

Hepatitis C virus (HCV) was characterized in 1989 as the organism responsible for non-A non-B hepatitis.² Because of an estimated 170 million people worldwide chronically infected with HCV, this virus represents a global public health problem. Approximately 80% of patients infected with HCV develop chronic hepatitis, which can lead to liver cirrhosis and hepatocellular carcinoma.³ Current standard-of-care of combination therapy with pegylated interferon-α and the nucleoside analogue ribavirin results in sustained virologic response (SVR) in only approximately 40–50% of patients with genotype 1.⁴ In contrast, SVR is achieved for greater than 80% of patients infected with genotypes 2 and 3 viruses. Thus, the greatest unmet medical need for HCV therapy is the improvement of SVR in genotype 1 patients.

The nonstructural protein 5B (NS5B) of HCV possesses RNA-dependent RNA polymerase (RdRp) activity essential for the repli-

cation of viral RNA genome, and exhibits the classic ‘right-hand’ configuration as other polymerases, with palm, thumb and finger subdomains.⁵ Intense drug discovery efforts have been directed toward the identification of potent and selective inhibitors of NS5B. Clinical proof-of-concept of NS5B polymerase inhibitors has been achieved with both nucleosides and non-nucleosides.⁶ Among nucleoside analogues, R7128 (Pharmasset/Roche)⁷ is currently the most advanced, followed by more recent inhibitors with improved in vitro potency such as IDX184 (Idenix)⁸ and PSI-7851 (Pharmasset).⁹ Clinical efficacy of a non-nucleoside inhibitor was first demonstrated with HCV-796 (ViroPharma/Wyeth) targeting the palm site,¹⁰ although further development of this compound was discontinued due to safety findings. Several structurally distinct palm site binders, however, have advanced into early clinical trials with encouraging results, for example, ABT-333 (Abbott)¹¹ and ANA598 (Anadys).¹² Compounds targeting other subdomains of NS5B are also undergoing clinical testing, such as thumb site binders PF-868554/filibuvir (Pfizer)¹³ and VX-222/VCH-222 (Vertex),¹⁴ and finger-loop site binder MK-3281 (Merck).¹⁵

In a continuing quest to discover novel HCV NS5B inhibitors, we initiated a hit characterization chemistry effort following high-throughput screening of a library of small molecules against NS5B using our proprietary ALIS (Automated Ligand Identification

* Corresponding author.

E-mail address: cccheng@alum.mit.edu (C.C. Cheng).

† Present address: Life Technologies, 5791 Van Allen Way, Carlsbad, CA 92008, United States.

‡ Present address: Aileron Therapeutics, Inc., 840 Memorial Dr., Cambridge MA 02139, United States.

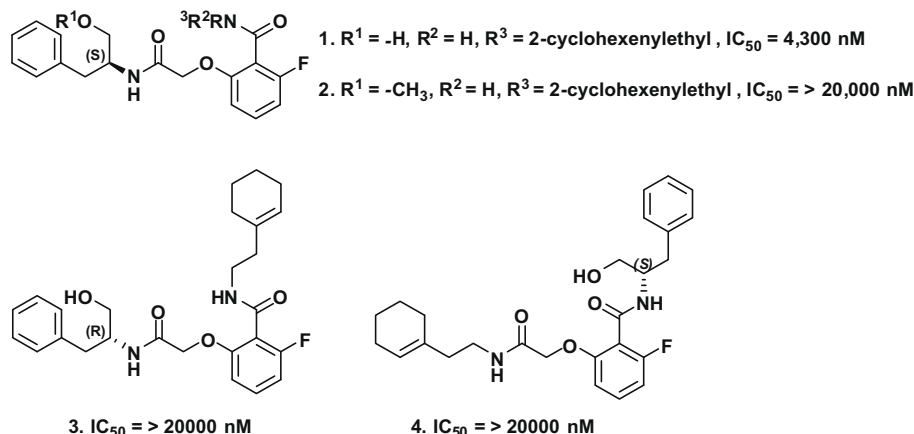


Figure 1. 2-Oxy-6-fluoro-*N*-((*S*)-1-hydroxy-3-phenylpropan-2-yl)-benzamide-based NS5B hits identified from ALIS screening.

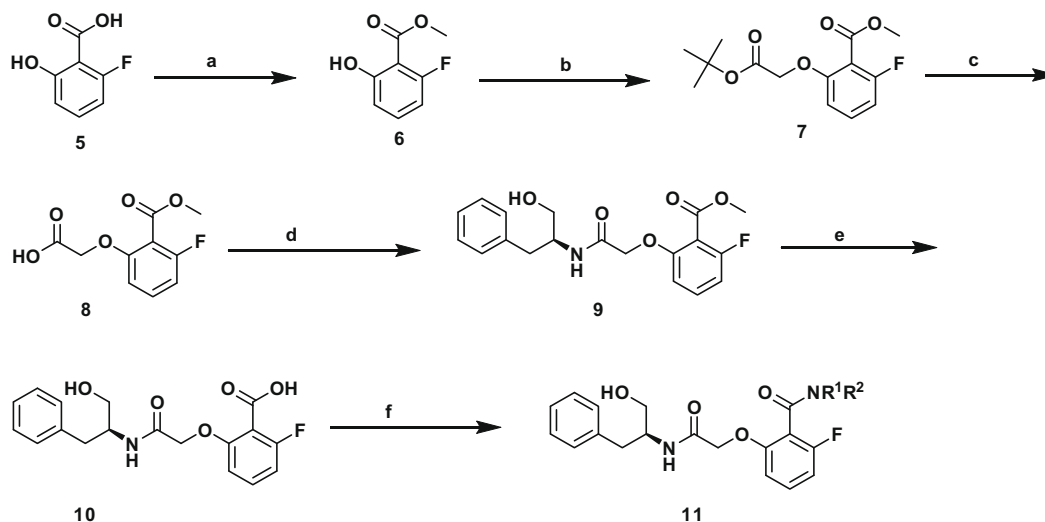
System) platform.¹ We describe herein the discovery and characterizations of potent and selective 2-oxy-6-fluoro-*N*-((*S*)-1-hydroxy-3-phenylpropan-2-yl)-benzamide-based NS5B inhibitors that were identified from mixture-based optimization of ALIS hits. We report our early mixture-based hit characterization efforts, using parallel synthesis and structure based drug design (SBDD), which led to the identification of submicromolar inhibitors of NS5B polymerase activity. Using X-ray crystallography and computer modeling we show an overlapping but distinct binding mode of this series of compounds from other palm site NNIs, consistent with biochemical characterization using enzyme mutants.

A hit characterization chemistry effort to find small molecule inhibitors targeting NS5B was initiated following high-throughput screening of NS5B($\Delta 21$)-genotype 1b (Con1) enzyme using the ALIS platform, an affinity selection-mass spectrometry platform for label-free, high-throughput screening of mixture-based combinatorial libraries. This screen revealed several classes of inhibitors, of which one (based on (*S*)-*N*-(2-cyclohexenylethyl)-2-fluoro-6-(2-(1-hydroxy-3-phenylpropan-2-ylamino)-2-oxoethoxy)benzamide (**1**), Fig. 1) is described herein. Interestingly, the lack of potency in the methoxy (**2**) and (*R*)-enantiomer (**3**) analogues suggested that the stereochemistry of the 1-hydroxy-3-phenylpropan-2-ylamide and hydrogen bond interactions with NS5B were important for

inhibition of enzyme activity.¹⁶ Further evidence of specificity was inferred when the two pendant amines of compound **1** were transposed as in compound **4** and a complete loss of potency resulted. These ligand–protein interactions were subsequently revealed upon the solution of the X-ray crystal structure of a representative complex described in detail below.

Preparation of key intermediates and final compounds in the 2-oxy-6-fluoro-*N*-((*S*)-1-hydroxy-3-phenylpropan-2-yl)-benzamide series began with methylation of 2-fluoro-6-hydroxybenzoic acid (**5**) as outlined in Scheme 1. Scaffolds such as **10** provided immediate access to SAR via hypothesis-driven ideas as well as more inclusive mixture-based synthetic libraries. Mixture-based libraries were analyzed using ALIS and provided both binary binding data as well as qualitative rank ordering.¹ Re-synthesis of the most promising hits was subsequently performed using high-throughput synthetic methods. Most notably a variety of amines (Table 1) was combined with the acid (**10**) to provide compounds **38–42** with a notable improvement in potency, quickly providing us with submicromolar inhibitors of NS5B.

Utilizing **1** as a starting point, we began the *in vitro* SAR characterizations by investigating the benzamides on the 6-fluorobenzoic acid (Table 1). From the early mixture-based optimization it was observed that the (*S*)-2-amino-3-phenylpropan-1-ol motif partici-



Scheme 1. Synthesis of (*S*)-2-fluoro-6-(2-(1-hydroxy-3-phenylpropan-2-ylamino)-2-oxoethoxy)benzoic acid and amidation. Reagents and conditions: (a) 2 equiv $TMSCH_2N_2$, MeOH, 0 °C; (b) 1 equiv *tert*-butyl bromoacetate, 1.5 equiv K_2CO_3 , DMF, rt, 18 h; (c) 9:1 TFA:H₂O, 2 h; (d) (*S*)-2-amino-3-phenylpropan-1-ol, HATU, DIEA, DMF, 12 h; (e) 1.5 equiv 1 N NaOH(aq), 1:1 MeOH–H₂O, then 1 N HCl(aq), 4 h; (f) NHR^1R^2 , 1.5 equiv 1,1'-carbonyldiimidazole, 1.5 equiv DIEA, NMP, 80 °C.

Table 1
SAR development of amides derived from intermediate **10**

Compd	NR ¹ R ²	NS5B IC ₅₀ ^{a,16} (μM)
12		>20
13		>20
14		>20
15		>20
16		>20
17		>20
18		>20
19		>20
20		>20
21		>20
22		>20
23		2.3
24		2.6
25		4
26		10
27		1.9
28		7.7
29		20
30		>20
31		20
32		0.43

Table 1 (continued)

Compd	NR ¹ R ²	NS5B IC ₅₀ ^{a,16} (μM)
33		4.3
34		4.6
35		8
36		6
37		17
38		>20
39		6
40		6
41		0.47
42		7
43		2.3
44		0.8
45		0.47
46		2.7
47		2.2
48		2.6

^a Values are means of duplicate experiments on two separate weightings.

pated in an essential H-bond network, confirmed by X-ray crystal structure with compound **44** (Fig. 2). Attempts to replace the cyclohexene ring with a saturated cyclohexane (**12**), phenyl (**13**) or with an H-bond accepting methoxy substituted (**14**) ring to de-couple or increase interactions with the adjacent Tyr-452 side chain were not tolerated and resulted in a significant loss of potency. Replacement of the cyclohexene ring with alkyl chains (**15–18**) to reduce possible steric interactions near the protein surface, add an H-bond donor (**19**) or a polar group (**20**) resulted in significant loss of potency. After further examination of the crystal structure and employing modeling techniques we observed that the adjacent Trp-550 was ~4.5 Å away from the N of the benzamide, suggesting that small substituents may be tolerated. Compounds (**21** and **22**) were made to test this hypothesis and unfortunately were inactive up to 20 μM. Surprisingly, both 4-methylcyclohexyl (**23**) and cycloheptyl (**24**) benzamides were tolerated. This may be due to the flexibility of NS5B protein at the binding site. Polar substituents on pyrrolidines (**28–30**) resulted in significant loss in potency relative to more hydrophobic substituents on the pyrrolidine amides (**25–27**) and affinity for NS5B may be due to the interactions with Trp-550. Since tertiary amides were somewhat tolerated we sought to explore tertiary amides analogues with linear alkyl chains (**35–48**). These groups provided good improvement in potency, whereas (*R*)-*N*-methyl-1-phenylethanamide (**32**),

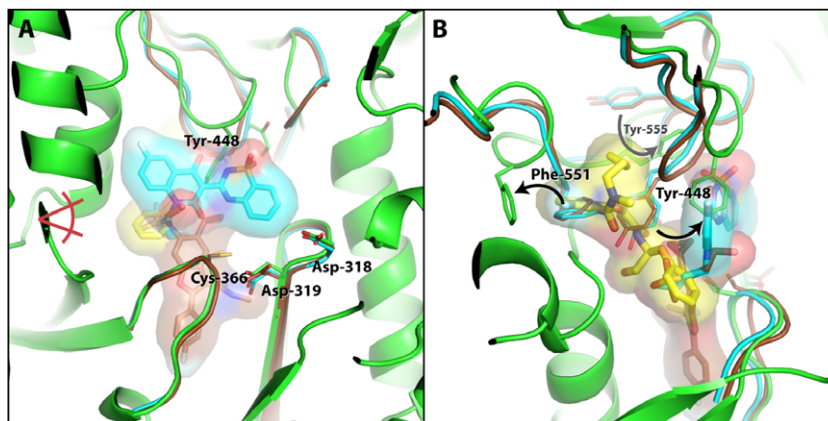


Figure 2. The complex containing HCV NS5B (green) and compound **44** (yellow) was superimposed with published structures containing binders at Palm Site 1 (cyan; PDB 2giq¹⁷) and Palm Site 2 (brown; PDB 3fqk¹⁸). Inhibitors are shown in stick representation with a transparent surface. Panel A (left) is a view into the active site cavity with the fingers subdomain to the right, the thumb subdomain to the left, and the palm subdomain at the bottom of the image. Asp-318 and Asp-319 do not move substantially among these three structures while Cys-366 shifts to form Palm Site 2. Viewing the Palm Site binders from the left side yields the view in Panel B (right). Compound **44** resides in a novel location denoted Palm Site 3, formed by a number of conformational changes, including a major shift Tyr-448 at the tip of the β -loop and a number of residues on the C-terminal portion of NS5B. Residues which undergo the largest rearrangements upon compound **44** binding are labeled, and arrows indicate the direction of the changes. This figure was prepared using PyMOL.¹⁹

N-methyl-3-methylbutylamide (**41**), and *N*-ethyl-butylamide (**45**) demonstrated submicromolar activity.

Compound **44** was found to bind within the active site cavity of NS5B near the top of the palm subdomain. Although proximal to the locations of a number of other published NS5B inhibitors,⁶ compound **44** binds in a distinct manner between the β -loop (residues 443–454) and the C-terminal tail region (551–555) in an almost completely enclosed cavity formed via significant shifts of both of those protein regions relative to other NS5B ligand complexes. This novel binding site is denoted Palm Site 3. Figure 2 illustrates the comparison of protein conformations and binding modes of compound **44** with Palm Site 1 (PDB code 2giq¹⁷) and Palm Site 2 (PDB code 3fqk¹⁸) binders.

Specific interactions between **44** and NS5B are detailed in Figure 3. An intramolecular hydrogen bond is observed between the carbonyl oxygen of the terminal amide and the nitrogen atom of the central amide. Intermolecular hydrogen bonds are observed from the carbonyl oxygen of the central amide both to a bound water molecule and to the side chain amide of Asn-316. Additional hydrogen bonding interactions are observed between the hydroxyl

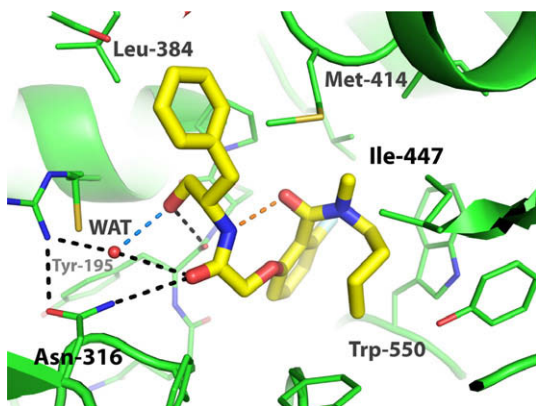


Figure 3. The crystal structure of NS5B (green) complexed with compound **44** (yellow). The intramolecular hydrogen bond is shown in orange. The intermolecular hydrogen bond from the inhibitor's hydroxyl group to the bound water molecule (labeled WAT) is shown in blue. The hydrogen bond network surrounding this water is shown in black. The coordinates have been deposited in the Protein Data Bank²⁰ with accession code 3lkh. This figure was prepared using PyMOL.¹⁹

group with the same bound water molecule as well as with the backbone carbonyl oxygen of Tyr-195. The remaining interactions are largely lipophilic and involve both aromatic and aliphatic protein side chains.

The binding mode of this compound is consistent with the observed SAR: while there is sufficient volume to accommodate the methoxy compound **2**, such an analogue juxtaposes the methoxy oxygen with the carbonyl oxygen of Tyr-195, leading to an unfavorable electrostatic mismatch. The (*S*) stereoisomer is essential in order to position the hydroxyl group within the hydrogen bonding network centered on the bound water molecule described above. Inversion of the chirality (**3**) leads to a polarity mismatch by placing the terminal benzyl group in a hydrophilic environment and the hydroxyl group in the lipophilic pocket between the side chains of Leu-384 and Met-414. Swapping of the terminal substituents (**4**) is sterically incompatible with the binding mode observed for compound **44**.

With respect to the SAR of amide substitution, the binding cavity presents a larger volume at the 'cis' side of the amide nitrogen. This observation accounts for the preference for *N,N*-disubstitution on the terminal amide to avoid the energetic penalty of a mono-substituted *cis*-amide.

Consistent with the binding interactions revealed in the X-ray crystal structure, the inhibitory potency of **44** was impacted by resistance mutations selected by known Palm Sites 1 and 2 binders. As shown in Table 2, there was an approximately 10-fold increase in IC₅₀ against a genotype 1b (Con1) NS5B variant containing a M414T change, and an even greater loss of potency against the C316Y (~100-fold) or G554D (~150-fold) variant. However, compound activity was unaffected by the C316N change. As expected, resistance mutations at the thumb site (M423T) or finger-loop site (P495L) did not reduce potency of this series of inhibitors (data not shown). The resistance profile of this class of inhibitors thus overlaps but is distinct from the previously described Palm Site 1 binder benzothiadiazine analogue A-848837²¹ or the Palm Site 2 binder benzofuran derivative HCV-796.^{10,18} Activity of neither compound was much affected by the M414T mutation, even though other inhibitors from the benzothiadiazine series have shown significant reduction in potency against this resistance locus. In contrast to compound **44**, HCV-796 activity was not changed by the G554D variant, which impacted A-848837 (~100-fold potency loss), consistent with

Table 2

Activity versus HCV NS5B enzyme variants

Compd	1b-Con1-IC ₅₀ , μM ^a	Con1-M414T IC ₅₀ , ^a μM	Con1-G554D IC ₅₀ , ^a μM	Con1-C316Y IC ₅₀ , ^a μM	Con1-C316N IC ₅₀ , ^a μM	1a IC ₅₀ , ^a μM
44	0.8	10	120	90	0.9	43
HCV-796	0.04	0.06	0.05	2	0.12	0.04
A-848837	0.003	0.004	0.3	0.008	0.004	0.003

^a Values are means of duplicate experiments on two separate weightings.

previous reports. However, HCV-796 activity was influenced by the polymorphism at residue 316, from a threefold increase in IC₅₀ against the N316 variant to a 50-fold increase against the Y316 variant versus its Con1 (C316) value. By comparison, compound **44** was sensitive to the C316Y but not the C316 N change, whereas A-848837 was unaffected by this resistance site.

With respect to the genotype spectrum of this series, compound **44** lost significant activity (50-fold) against a genotype 1a enzyme, and was not active up to 200 μM against genotypes 2, 3, and 4 (data not shown). In contrast, HCV-796 and A-848837 demonstrated equal potency against 1a and 1b genotypes; HCV-796 in particular has shown broad activity across multiple genotypes.¹⁰

To further investigate the mechanism of action of this novel series of NS5B inhibitors, we performed a single-round elongation assay as described previously¹⁶ to determine if these compounds inhibit at the initiation or the elongation step. As shown in Figure 4, while compound **44** was fully active (IC₅₀ = 0.6 μM) against primer-initiated RNA synthesis involving multiple cycles of initiation and elongation catalyzed by NS5B, it was ineffective (IC₅₀ > 200 μM) in inhibiting the elongation of preformed NS5B enzyme–primer–template complexes. Thus, these compounds appeared to act as inhibitors of initiation of replication, as observed with other allosteric non-nucleoside NS5B inhibitors which bind in this vicinity.²²

Selected compounds from this series were also tested against BVDV and poliovirus polymerases as well as host polymerases DNA pol-α, -β, -γ; all showed excellent selectivity (inactive up to 200 μM). However, none of the compounds in this series have so far demonstrated activity in the cell-based HCV subgenomic replicon system up to 25 μM (data not shown).

In summary, we have described a novel series of HCV NS5B inhibitors based on the 2-oxy-6-fluoro-N-((S)-1-hydroxy-3-phenylpropan-2-yl)-benzamide-based scaffold. Beginning with relatively weak hits from the ALIS platform, we were able to rapidly identify inhibitors with improved potency in the submicromolar range by combining mixture-based optimization with computer-aided design. The X-ray crystal structure of a complex with a representative compound has provided structural insights

into the mechanism of inhibition and rationalization of the SAR. Biochemical characterizations have further elucidated the mechanism of inhibition of this new class of NS5B inhibitors. It is believed that further structural modifications such as rigidification may improve cell penetration and yield compounds with anti-HCV replicon activity. Future lead optimization efforts focusing on broadened genotype coverage and suitable pharmacokinetics and ancillary properties may lead to the identification of a clinical candidate for the treatment of hepatitis C.

Acknowledgments

We thank Dr. Xianshu Yang for performing the initial ALIS screening, Michael Starks for analytical support, Zhiqing He and Patricia McMonagle for generating the NS5B enzyme constructs.

References and notes

- (a) Annis, D. A.; Athanasopoulos, J.; Curran, P. J.; Felsch, J. S.; Kalghatgi, K.; Lee, W. H.; Nash, H. M.; Orminati, J.-P.; Rosner, K. E.; Shipps, G. W., Jr. *Int. J. Mass Spectrom.* **2004**, *238*, 77; (b) Annis, D. A.; Nickbarg, E. B.; Yang, X.; Ziebell, M. R.; Whitehurst, C. E. *Curr. Opin. Chem. Biol.* **2007**, *11*, 518; (c) Annis, D. A.; Shipps, G. W., Jr.; Deng, Y.; Popovici-Muller, J.; Siddiqui, M. A.; Curran, P. J.; Gowen, M.; Windsor, W. T. *Anal. Chem.* **2007**, *79*, 4538; (d) Shipps, G. W., Jr.; Deng, Y.; Wang, T.; Popovici-Muller, J.; Curran, P. J.; Rosner, K. E.; Cooper, A. B.; Girijavallabhan, V.; Butkiewicz, N.; Cable, M. *Bioorg. Med. Chem. Lett.* **2005**, *15*, 115.
- Choo, Q. L.; Kuo, G.; Weiner, A. J.; Overby, L. R.; Bradley, D. W.; Houghton, M. *Science* **1989**, *244*, 359.
- Alter, H. J.; Seeff, L. B. *Semin. Liver Dis.* **2000**, *20*, 17.
- (a) Manns, M. P.; McHutchison, J. G.; Gordon, S. C.; Rustgi, V. K.; Shiffman, M.; Reindollar, R.; Goodman, Z. D.; Koury, K.; Ling, M.; Albrecht, J. K. *Lancet* **2001**, *358*, 958; (b) Fried, M. W.; Shiffman, M. L.; Reddy, K. R.; Smith, C.; Marinos, G.; Goncalves, F. L., Jr.; Haussinger, D.; Diago, M.; Carosi, G.; Dhumeaux, D.; Craxi, A.; Lin, A.; Hoffman, J.; Yu, J. N. *Eng. J. Med.* **2002**, *347*, 975.
- (a) Lesburg, C. A.; Cable, M. B.; Ferrari, E.; Hong, Z.; Mannarino, A. F.; Weber, P. C. *Nat. Struct. Biol.* **1999**, *6*, 937; (b) Bressanelli, S.; Tomei, L.; Roussel, A.; Incitti, I.; Vitale, R. L.; Mathieu, M.; De Francesco, R.; Rey, F. A. *Proc. Natl. Acad. Sci. U.S.A.* **1999**, *96*, 13034; (c) Ago, H.; Adachi, T.; Yoshida, A.; Yamamoto, M.; Habuka, N.; Yatsunami, K.; Miyano, M. *Structure* **1999**, *7*, 1417.
- (a) Beaulieu, P. L. *Expert. Opin. Ther. Patents* **2009**, *19*, 145; (b) Koch, U.; Narjes, F. *Curr. Top. Med. Chem.* **2007**, *7*, 1302; (c) Carroll, S. S.; Olsen, D. B. *Infect. Disord. Drug Targets* **2006**, *6*, 17.
- Lalezari, J.; Gane, E.; Rodriguez-Torres, M.; De Jesus, E.; Nelson, D.; Everson, G.; Jacobson, I.; Reddy, R.; Hill, G. Z.; Beard, A.; Symonds, W. T.; Berrey, M. M.; McHutchison, J. G. *J. Hepatol.* **2008**, *48*, S29.
- Cretton-Scott, E.; Perigaud, C.; Peyrottes, S.; Licklider, L.; Camire, M.; Larsson, M.; La Colla, M.; Hildebrand, E.; Lallous, L.; Bilello, J.; McCarville, J.; Seifer, M.; Liuzzi, M.; Pierra, C.; Badaroux, E.; Gosselin, G.; Surleraux, D.; Standring, D. N. *J. Hepatol.* **2008**, *48*, S220.
- Furman, P. A.; Wang, P.; Niu, C.; Bao, D.; Symonds, W.; Nagarathnam, D.; Steuer, H. M.; Rachakonda, S.; Ross, B. S.; Otto, M. J.; Sofia, M. J. *Hepatol.* **2008**, *48*, 1161A.
- (a) Howe, A. Y.; Cheng, H.; Johann, S.; Mullen, S.; Chunduru, S. K.; Young, D. C.; Bard, J.; Chopra, R.; Krishnamurthy, G.; Mansour, T.; O'Connell, J. *Antimicrob. Agents Chemother.* **2008**, *52*, 3327; (b) Kneteman, N. M.; Howe, A. Y.; Gao, T.; Lewis, J.; Pevear, D.; Lund, G.; Douglas, D.; Mercer, D. F.; Tyrrell, D. L.; Immermann, F.; Chaudhary, I.; Speth, J.; Villano, S. A.; O'Connell, J.; Collett, M. J. *Hepatol.* **2009**, *49*, 745.
- Rodriguez-Torres, M.; Lawitz, E.; Cohen, D.; Larsen, L. M.; Menon, R.; Collins, C.; Marsh, T.; Gibbs, S.; Bernstein, B. *J. Hepatol.* **2009**, *50*, 91A.
- Lawitz, E.; Rodriguez-Torres, M.; DeMicco, M.; Nguyen, T.; Godofsky, E.; Appleman, J.; Rahimy, M.; Crowley, C.; Fredro, J. *J. Hepatol.* **2009**, *50*, S384.
- Jacobson, I.; Pockros, P.; Lalezari, J.; Lawitz, E.; Rodriguez-Torres, M.; Dejesus, E.; Haas, F.; Martorell, C.; Pruiett, R.; Durham, K.; Srinivasan, S.; Rosario, M.; Jagannatha, S.; Hammond, J. *J. Hepatol.* **2009**, *50*, S382.
- Cooper, C.; Larouche, R.; Bourgalet, B.; Charet, N.; Proulx, L. *J. Hepatol.* **2009**, *50*, S342.

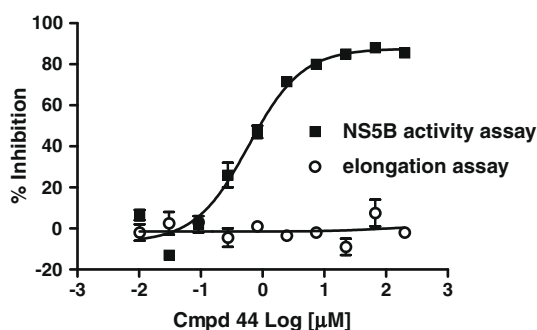


Figure 4. Mechanism of action of compound **44**. NS5B activity assay measured multiple rounds of initiation and primer-extension, whereas the elongation assay measured the burst phase activity consisting of single-round extension of enzyme–primer–template after preincubation.¹⁶

15. Brainard, D. M.; Anderson, M. S.; Petry, A.; Van Dyck, K.; De Lepeleire, I.; Sneddon, K.; Cummings, C. E.; Nachbar, R. B.; Barnard, R. J.; Sun, P.; Panorchan, P.; Sanderson, J. B.; Udezue, E.; Wagner, F.; Iwamoto, M.; Chodakewitz, J.; Wagner, J. A. *J. Hepatol.* **2009**, *50*, 1026A.
16. Ferrari, E.; He, Z.; Palermo, R. E.; Huang, H. C. *J. Biol. Chem.* **2008**, *283*, 33893. HCV NS5B polymerase activity was measured in a radiolabeled nucleotide incorporation assay as follows: 50 μ L reactions containing 20 mM HEPES (pH 7.3), 7.5 mM DTT, 20 units/mL RNasin, 1 μ M GTP, ATP and UTP, 60 μ Ci/mL [32 P]-CTP supplemented to 20 nM CTP, 10 mM MgCl₂, 60 mM NaCl, 100 μ g/mL BSA, 100 nM heteropolymer RNA template, 0.25 mM trinucleotide initiator and 30 nM NS5B (Δ 21) enzyme were incubated at room temperature for 2 h. Assay was terminated by the addition of 50 μ L 500 mM EDTA. The reaction mixture was transferred to Millipore DE81 filter plate and the incorporation of labeled CTP was determined by Packard TopCount. For primer-initiated RNA synthesis, the trinucleotide initiator was replaced by 100 nM of an 11-mer RNA primer complementary to the 3'-end of the RNA template. Single-round elongation reaction was performed at room temperature for 15 min using enzyme, primer and template complex preincubated at room temperature for 22 h. Compound IC₅₀ values were calculated from experiments with 10 serial twofold dilutions of the inhibitor in duplicate.
17. Le Pogam, S.; Kang, H.; Harris, S. F.; Leveque, V.; Giannetti, A. M.; Ali, S.; Jiang, W. R.; Rajyaguru, S.; Tavares, G.; Oshiro, C.; Hendricks, T.; Klumpp, K.; Symons, J.; Browner, M. F.; Cammack, N.; Najera, I. *J. Virol.* **2006**, *80*, 6146.
18. Hang, J. Q.; Yang, Y.; Harris, S. F.; Leveque, V.; Whittington, H. J.; Rajyaguru, S.; Ao-leong, G.; McCown, M. F.; Wong, A.; Giannetti, A. M.; Le Pogam, S.; Talamas, F.; Cammack, N.; Najera, I.; Klumpp, K. *J. Biol. Chem.* **2009**, *284*, 15517.
19. Delano, W. L. *The PyMOL Molecular Graphics System*; DeLano Scientific: San Carlos, CA, 2002.
20. Berman, H. M.; Westbrook, J.; Feng, Z.; Gilliland, G.; Bhat, T. N.; Weissig, H.; Shindyalov, I. N.; Bourne, P. E. *Nucleic Acids Res.* **2000**, *28*, 235.
21. (a) Mo, H.; Lu, L.; Pilot-Matias, T.; Pithawalla, R.; Mondal, R.; Masse, S.; Dekhtyar, T.; Ng, T.; Koev, G.; Stoll, V.; Stewart, K. D.; Pratt, J.; Donner, P.; Rockway, T.; Maring, C.; Molla, A. *Antimicrob. Agents Chemother.* **2005**, *49*, 4305; (b) Lu, L.; Dekhtyar, T.; Masse, S.; Pithawalla, R.; Krishnan, P.; He, W.; Ng, T.; Koev, G.; Stewart, K.; Larson, D.; Bosse, T.; Wagner, R.; Pilot-Matias, T.; Mo, H.; Molla, A. *Antiviral Res.* **2007**, *76*, 93.
22. Liu, Y.; Jiang, W. W.; Pratt, J.; Rockway, T.; Harris, K.; Vasavanonda, S.; Tripathi, R.; Pithawalla, R.; Kati, W. M. *Biochemistry* **2006**, *45*, 11312.